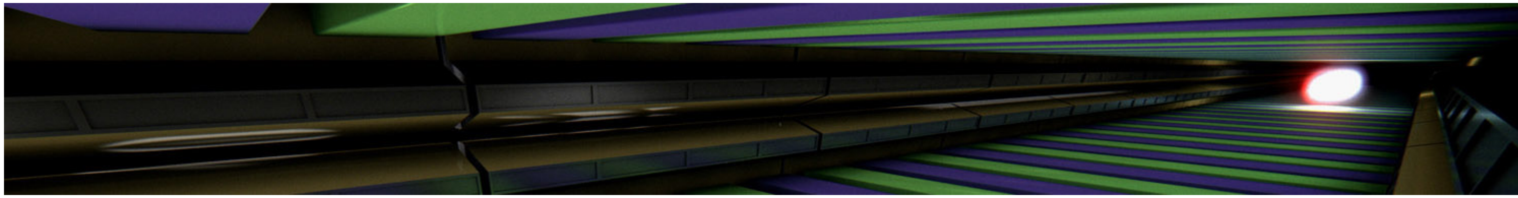

Fundamental Limitations of the SASE FEL Photon Beam Pointing Stability

E.A. Schneidmiller and M.V. Yurkov

FEL Seminar, November 17, 2015

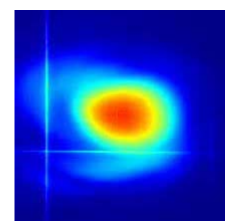

- General overview of coherence properties.
- Eigenmodes and eigenfunctions.
- Experience from FLASH.
- Optimized x-ray FEL.
- Coherence properties of the radiation from optimized x-ray FEL.
- Photon beam pointing stability.

Statistical properties of the radiation / impact on user experiments /

Poor longitudinal coherence:

- Fluctuations of the instantaneous intensity;
- Fluctuations of the energy in the radiation pulse;
- Uncorrelated fields along radiation pulse due to limited coherence time

Poor transverse coherence:

- Uncorrelated fields across radiation pulse;
- Poor pointing stability;
- Essentially non-gaussian slice field patterns.

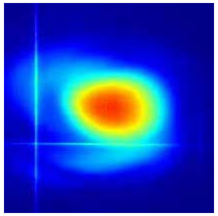

SASE FEL

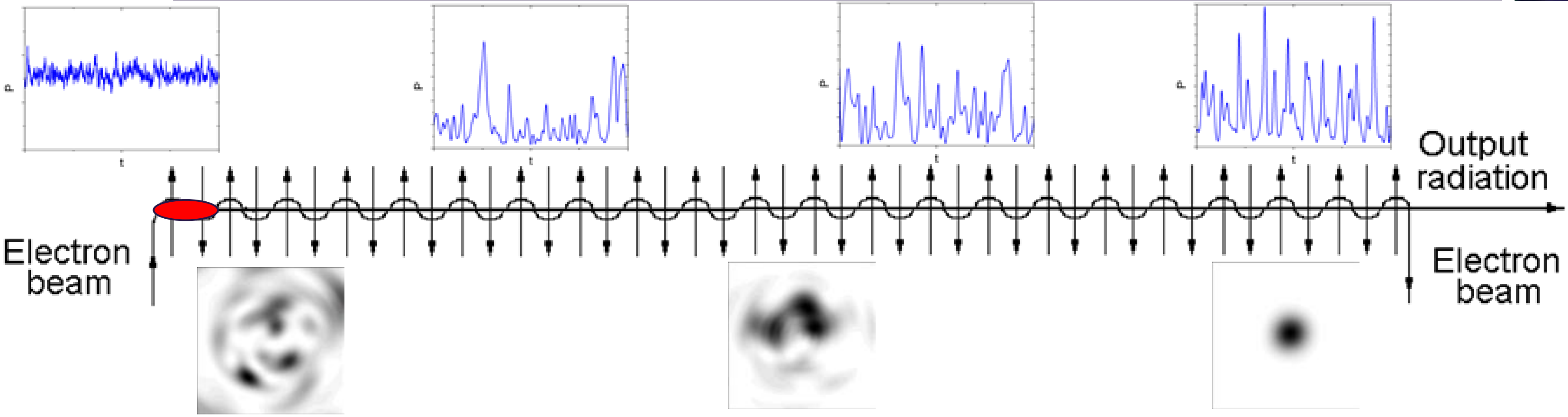

- Fluctuations of current density in the electron beam are uncorrelated not only in time but in space, too.
- When the electron beam enters the undulator, the presence of the beam modulation at frequencies close to the resonance frequency initiates the process of amplification. Radiation generated by SASE FEL consists of wavepackets (spikes).
- A large number of transverse radiation modes are excited when the electron beam enters the undulator.
- These radiation modes have different gain. As undulator length progresses, the high gain modes will predominate more and more and we can regard the XFEL as filter, in the sense that it filters from arbitrary radiation field those components corresponding to the high gain modes.

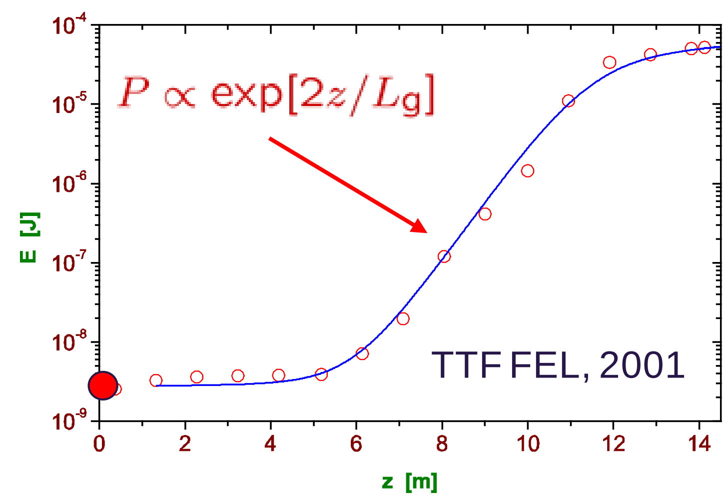

Statistics and probability distributions

Linear regime	Saturation	Deep nonlinear regime

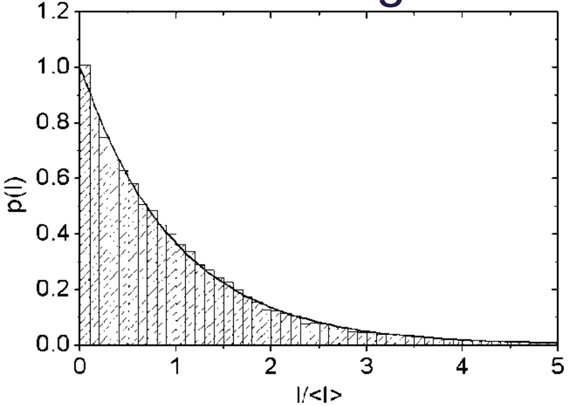

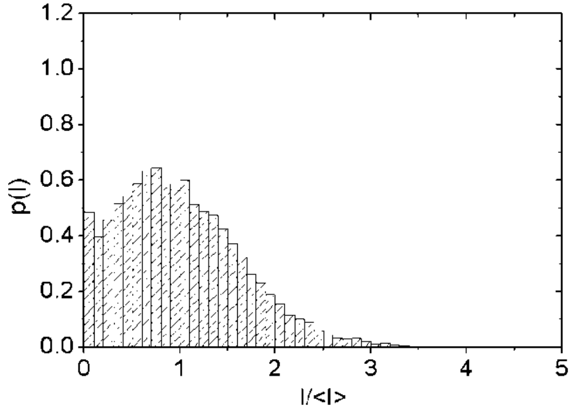

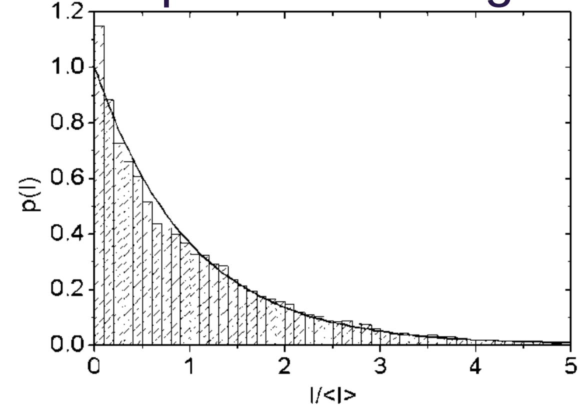

- Probability distributions of the instantaneous power density (top) and of the instantaneous radiation power (bottom) look more elegant and seem to be described by simple functions.

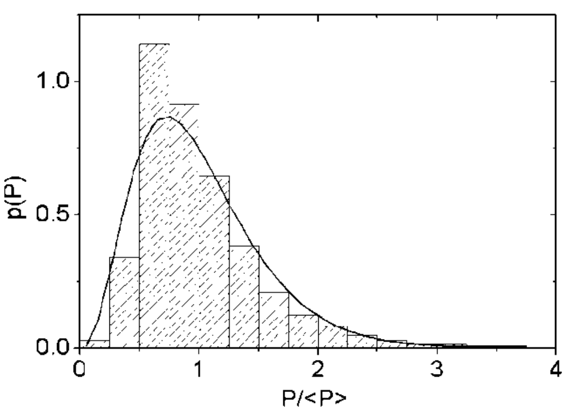

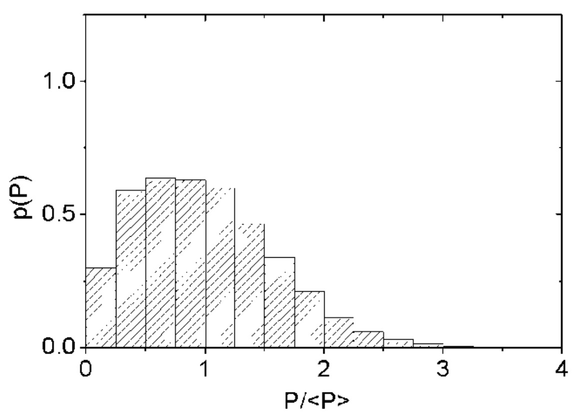

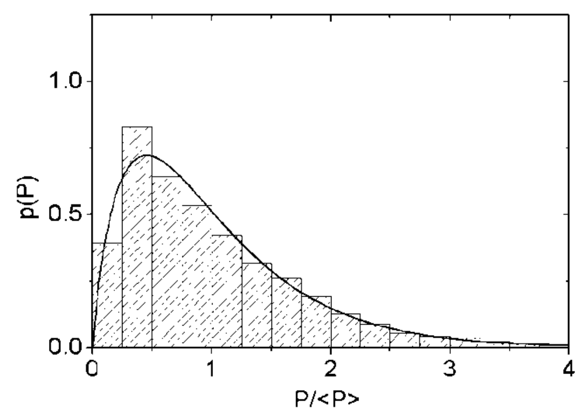

Statistics and probability distributions

Radiation from SASE FEL operating in the high gain linear regime possesses all the features of completely chaotic polarized light:

- The higher order correlation functions are expressed via the first order correlation function

$$g_2(t-t') = 1 + |g_1(t-t')|^2 \,, \qquad g_2(\Delta\omega) = 1 + |g_1(\Delta\omega)|^2$$

- The probability density distribution of the instantaneous radiation power $p(P)$ follows the negative exponential distribution, and the probability density function of the finite-time integrals of the instantaneous power and of the radiation energy after monochromator $p(W)$ follows the gamma distribution:

$$p(P) = \frac{1}{<P>} \exp\left(-\frac{P}{<P>}\right) \,, \qquad p(W) = \frac{M^M}{\Gamma(M)} \left(\frac{W}{<W>}\right)^{M-1} \frac{1}{<W>} \exp\left(-M\frac{W}{<W>}\right) \,,$$

- Parameter M has physical sense of the number of modes in the radiation pulse:

$$M^{-1} = \sigma_W^2 =< (W- < W >)^2 > / < W >^2$$

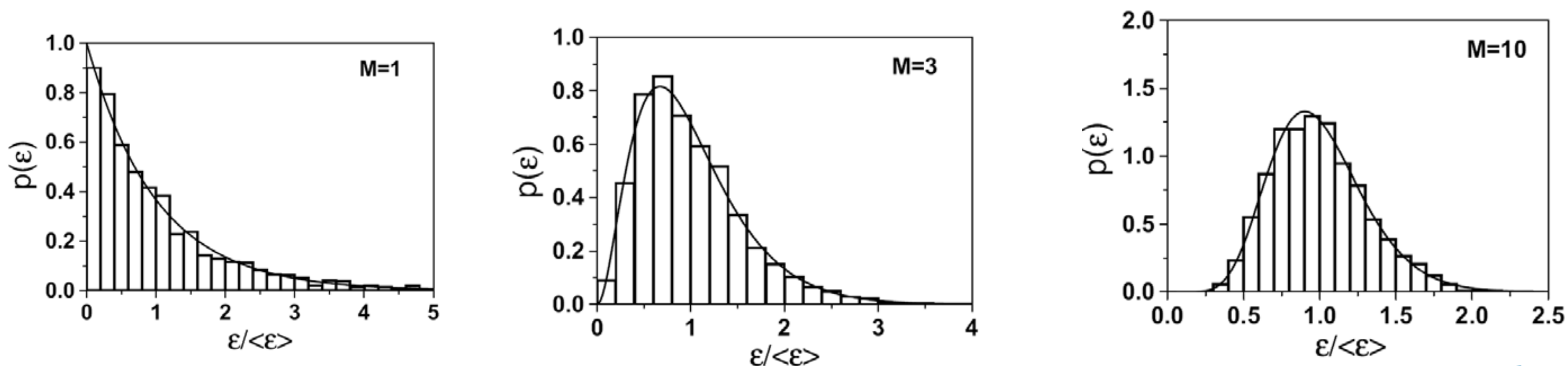

Strict definitions of statistical characteristics

- The first order time correlation function and coherence time:

$$g_1(\vec{r}, t - t') = \frac{\langle \tilde{E}(\vec{r}, t)\tilde{E}^*(\vec{r}, t')\rangle}{\left[\langle |\ \tilde{E}(\vec{r}, t)\ |^2\rangle\langle |\ \tilde{E}(\vec{r}, t')\ |^2\rangle\right]^{1/2}} \ , \qquad \tau_c = \int\limits_{-\infty}^{\infty} |g_1(\tau)|^2 \, \mathrm{d}\,\tau \ .$$

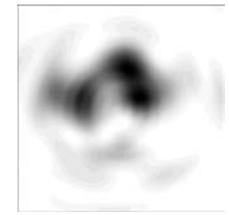

- The first-order transverse correlation function and degree of transverse coherence:

$$\gamma_1(\vec{r}_\perp, \vec{r\prime}_\perp, z, t) = \frac{\langle \tilde{E}(\vec{r}_\perp, z, t)\tilde{E}^*(\vec{r\prime}_\perp, z, t)\rangle}{\left[\langle |\tilde{E}(\vec{r}_\perp, z, t)|^2\rangle\langle |\tilde{E}(\vec{r\prime}_\perp, z, t)|^2\rangle\right]^{1/2}} \ .$$

$$\zeta = \frac{\int\int |\gamma_1(\vec{r}_\perp, \vec{r\prime}_\perp)|^2 \langle I(\vec{r}_\perp)\rangle\langle I(\vec{r\prime}_\perp)\rangle \, \mathrm{d}\,\vec{r}_\perp \, \mathrm{d}\,\vec{r\prime}_\perp}{\left[\int \langle I(\vec{r}_\perp)\rangle \, \mathrm{d}\,\vec{r}_\perp\right]^2} \ .$$

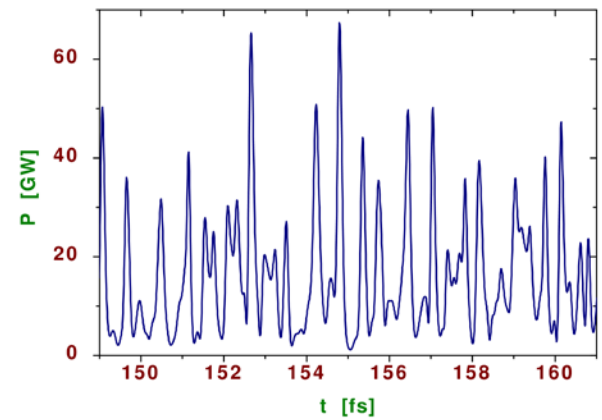

- Degeneracy parameter – the number of photons per mode:

$$\delta = \dot{N}_{ph}\tau_c\zeta \ .$$

- Peak brilliance is defined as a transversely coherent spectral flux:

$$B_r = \frac{\omega \, \mathrm{d}\,\dot{N}_{ph}}{\mathrm{d}\,\omega} \frac{\zeta}{\left(\frac{\lambda}{2}\right)^2} = \frac{4\sqrt{2}c}{\lambda^3}\,\delta \ .$$

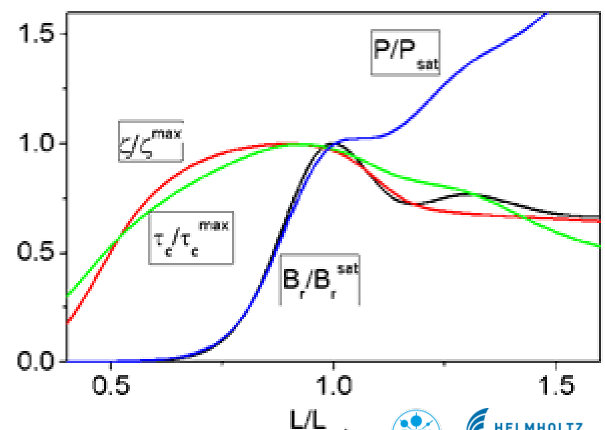

Qualitative outlook of transverse coherence

Degree of transverse coherence

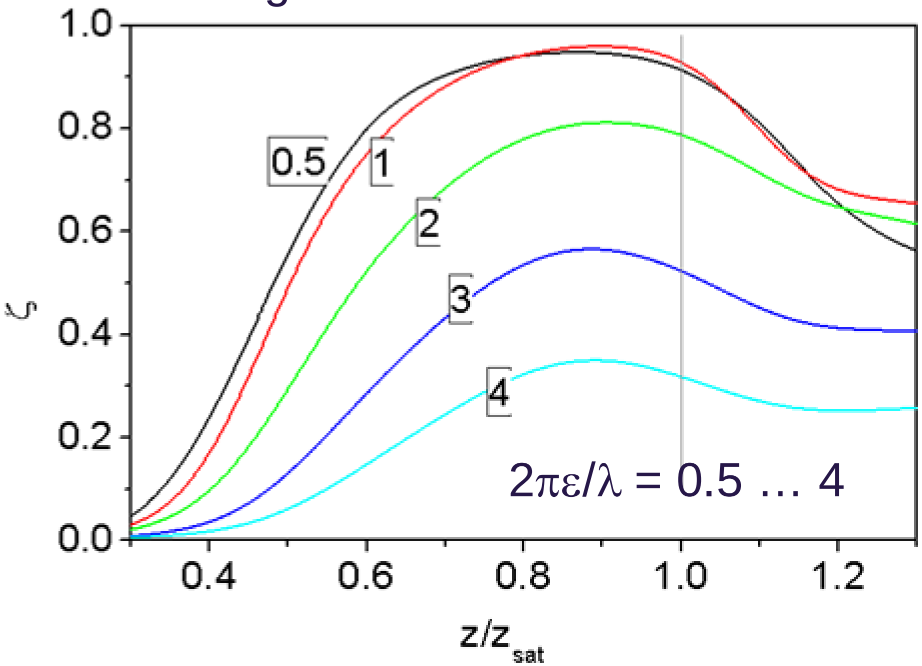

z-s intensity distribution

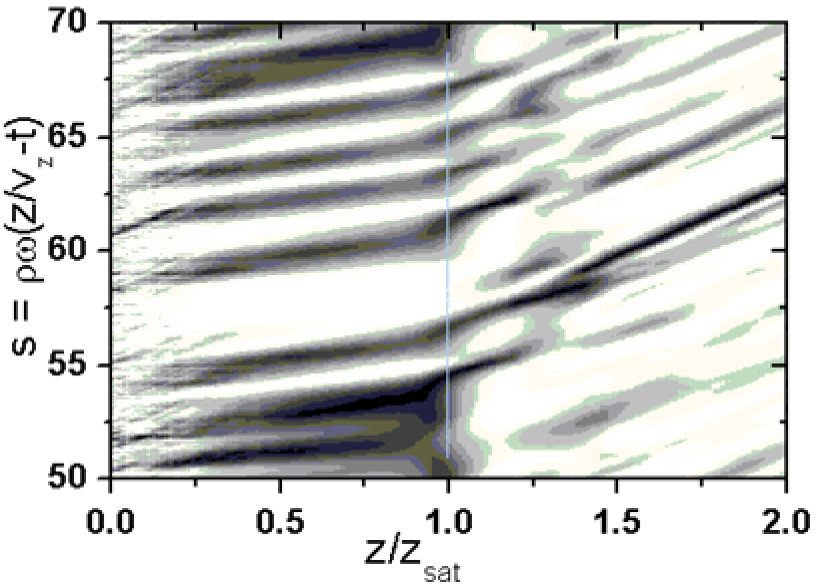

- For small emittances the degree of transverse coherence visibly differs from unity. This happens due to poor longitudinal coherence: radiation spikes move forward along the electron beam, and interact with those parts of the beam which have different amplitude/phase.
- Degradation of the longitudinal coherence leads to significant degradation of the transverse coherence in the post-saturation regime.

Qualitative outlook of transverse coherence

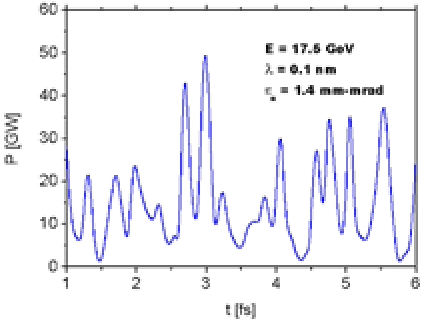

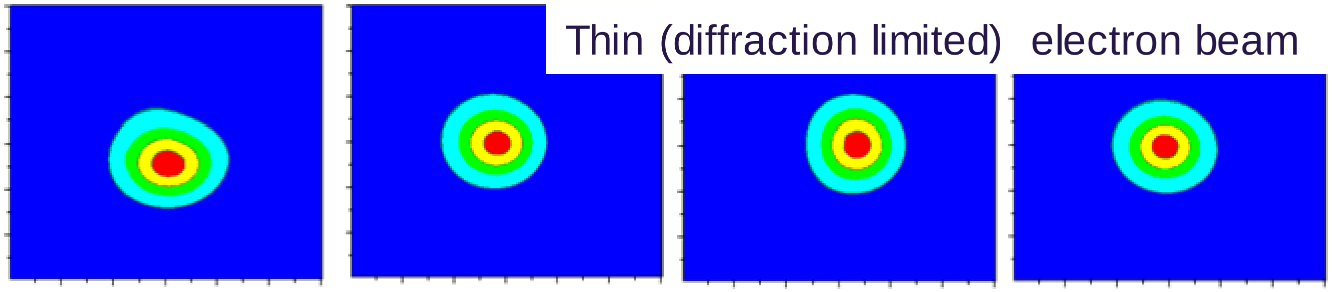

Thin (diffraction limited) electron beam

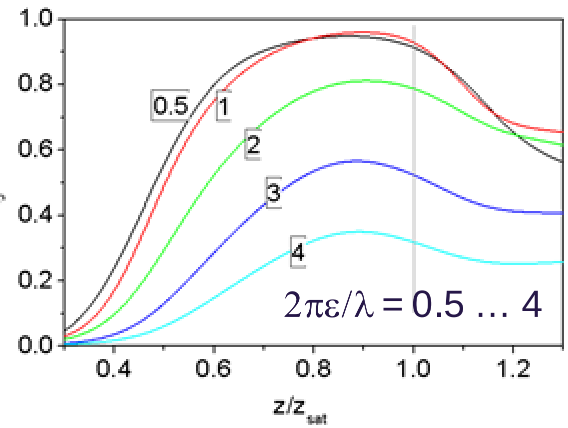

- Undulator length to saturation is limited (9 to 10 field gain length for X-ray FELs).
- In the case of wide electron beam (with transverse size larger than diffraction expansion of the radiation on the scale of the field gain length) , the degree of transverse coherence degrades due to poor mode selection.

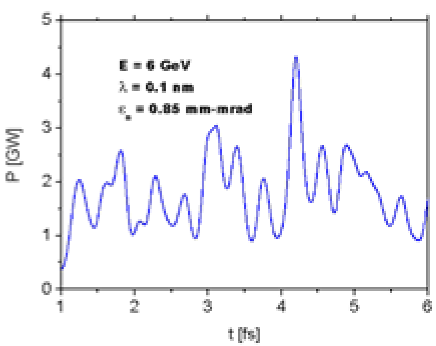

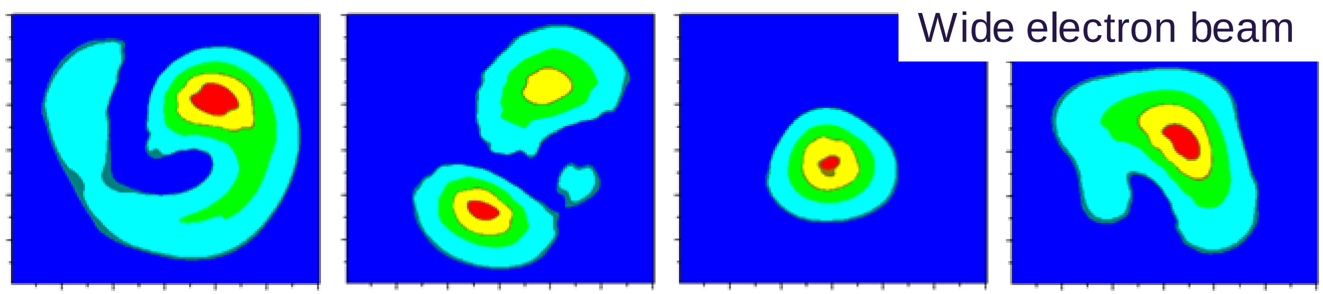

Wide electron beam

Outline

- General overview of coherence properties.
- Eigenmodes and eigenfunctions.
- Experience from FLASH.
- Optimized x-ray FEL.
- Coherence properties of the radiation from optimized x-ray FEL.
- Photon beam pointing stability.

Self-reproducing FEL radiation modes

- In the linear high-gain limit the radiation emitted by the electron beam in the undulator can be represented as a set of modes:

$$E_{\mathrm{x}} + iE_{\mathrm{y}} = \int \mathrm{d}\omega \exp[i\omega(z/c - t)] \times \sum_{n,k} A_{nk}(\omega, z)\Phi_{nk}(r, \omega) \exp[\Lambda_{nk}(\omega)z + in\phi] \, .$$

- A large number of transverse radiation modes are excited when the electron beam enters the undulator. These radiation modes have different gain. As undulator length progresses, the fundamental Φ_{00} mode predominate more and more over higher spatial modes.

- Parameter space of long wavelength x-ray FELs corresponds to the case of diffraction limited electron beams. Radiation modes in this case are well separated in the gain, and it is possible to obtain a high degree of transverse coherence in the saturation point.

- Parameter space of short wavelength XFELs correspond to the case of the wide electron beam, and the mode degeneration effect prevents suppression of higher spatial modes. The consequences are:
  - Degradation of transverse coherence;
  - Poor pointing stability;
  - Complicated and essentially non-gaussian field distributions across the slices of the radiation pulse which happens due to interference of many statistically independent spatial modes.

- These effects stems from fundamental origin - start-up of the amplification process from the shot noise in the electron beam.

Self-reproducing FEL radiation modes

$$
\begin{aligned}
&\left[\frac{\mathrm{d}^2}{\mathrm{d}\hat{r}^2}+\frac{1}{\hat{r}}\frac{\mathrm{d}}{\mathrm{d}\hat{r}}-\frac{n^2}{\hat{r}^2}+2\mathrm{i}B\hat{\Lambda}\right]\Phi_n(\hat{r}) \\
&= -4\int_0^\infty d\hat{r}'\,\hat{r}'\,\{\Phi_n(\hat{r}') \qquad\qquad (4)\\
&\quad +\frac{\hat{\Lambda}_{\mathrm{p}}^2}{2}\left[\frac{\mathrm{d}^2}{\mathrm{d}\hat{r}'^2}+\frac{1}{\hat{r}'}\frac{\mathrm{d}}{\mathrm{d}\hat{r}'}-\frac{n^2}{\hat{r}'^2}+2\mathrm{i}B\hat{\Lambda}\right]\Phi_n(\hat{r}')\Bigg\} \\
&\quad \times\int_0^\infty \mathrm{d}\zeta\frac{\zeta}{\sin^2(\hat{k}_\beta\zeta)}\exp\left[-\frac{\hat{\Lambda}_T^2\zeta^2}{2}-(\hat{\Lambda}+\mathrm{i}\hat{C})\zeta\right] \\
&\quad \times\exp\left[-\frac{(1-\mathrm{i}B\hat{k}_\beta^2/2)(\hat{r}^2+\hat{r}'^2)}{\sin^2(\hat{k}_\beta\zeta)}\right] \\
&\quad \times I_n\left[\frac{2(1-\mathrm{i}B\hat{k}_\beta^2\zeta/2)\hat{r}\hat{r}'\cos(\hat{k}_\beta\zeta)}{\sin^2(\hat{k}_\beta\zeta)}\right]
\end{aligned}
$$

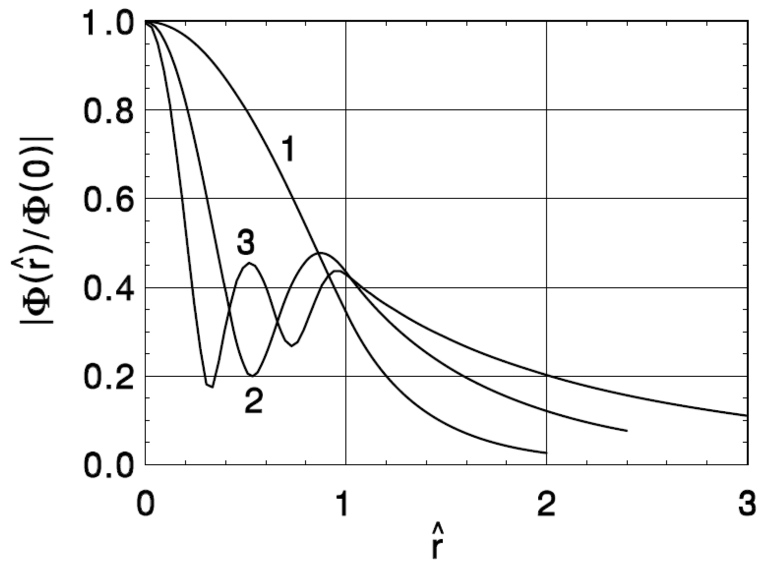

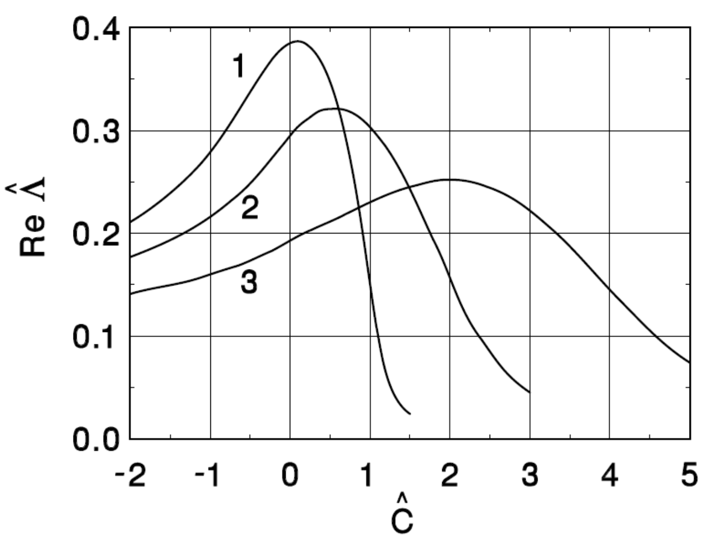

Analytical techniques are used to calculate radiation fields in the linear mode of operation, and time-dependent numerical simulation codes are used in the general case.

Mode degeneration

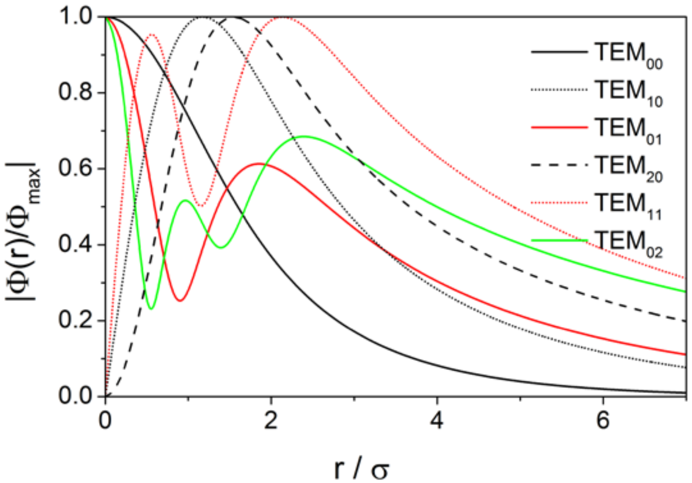

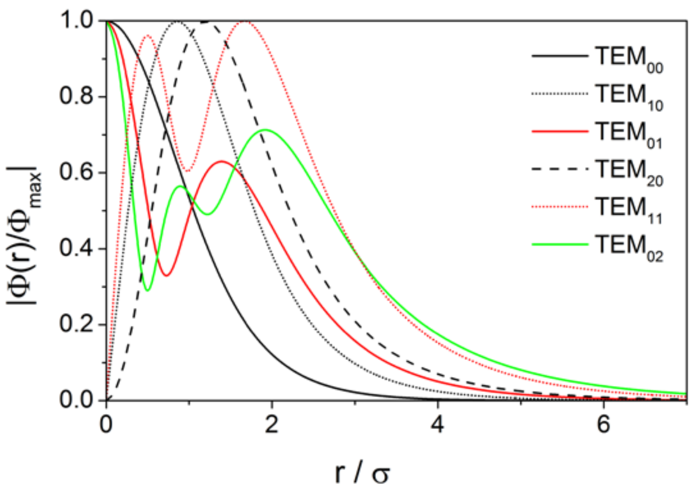

Eigenfunctions for B = 1 and B = 10

- Operation of the FEL amplifier is described by the diffraction parameter B, the energy spread parameter $\hat{\Lambda}^2_{\mathrm{T}}$, and the betatron motion parameter $\hat{k}_\beta$:

$$B = 2\Gamma\sigma^2\omega/c\ , \qquad \hat{k}_\beta = 1/(\beta\Gamma)\ , \qquad \hat{\Lambda}^2_{\mathrm{T}} = (\sigma_{\mathrm{E}}/\mathcal{E})^2/\rho^2\ ,$$

with the gain parameter $\Gamma = 4\pi\rho/\lambda_w$.

- An effect of the mode degeneration takes place for large values of the diffraction parameter B:

$$\Lambda_{mn}/\Gamma \simeq \frac{\sqrt{3}+\mathrm{i}}{2B^{1/3}} - \frac{(1+\mathrm{i}\sqrt{3})(1+n+2m)}{3\sqrt{2}B^{2/3}}$$

- The strongest higher order spatial mode is the first azimuthally nonsymmetric mode TEM_{10} mode.

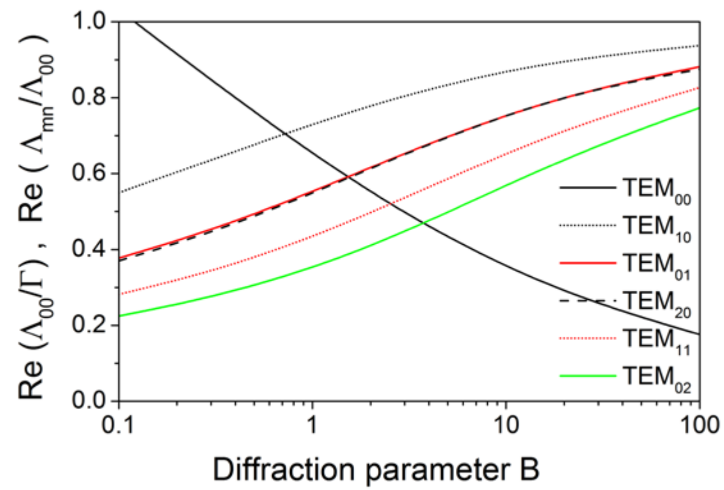

Mode degeneration

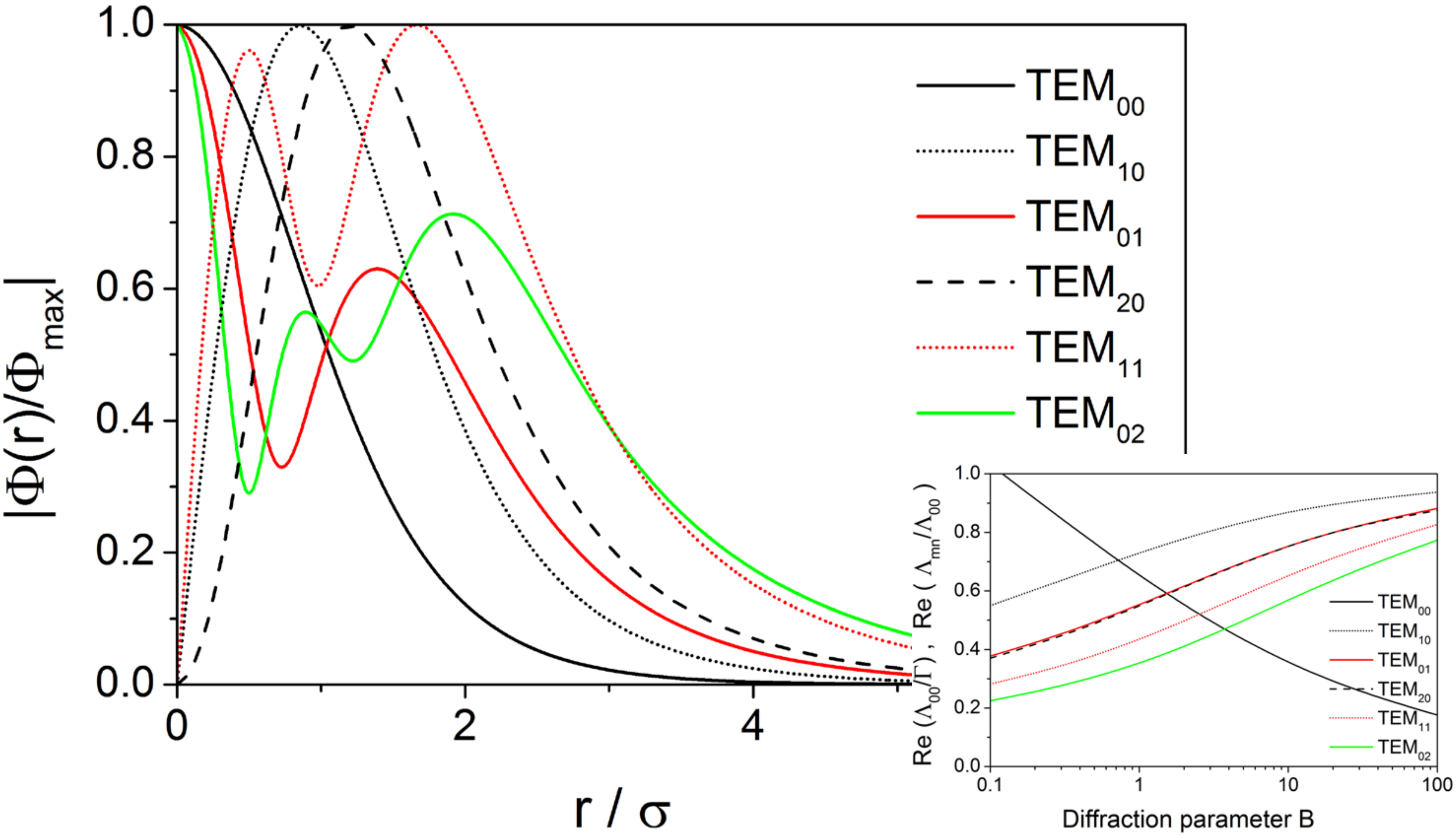

Eigenfunctions for B = 10

Mode degeneration

- Operation of the FEL amplifier is described by the diffraction parameter B, the energy spread parameter $\hat{\Lambda}^2_{\mathrm{T}}$, and the betatron motion parameter $\hat{k}_\beta$:

$$B = 2\Gamma\sigma^2\omega/c \ , \qquad \hat{k}_\beta = 1/(\beta\Gamma) \ , \qquad \hat{\Lambda}^2_{\mathrm{T}} = (\sigma_{\mathrm{E}}/\mathcal{E})^2/\rho^2 \ ,$$

with the gain parameter $\Gamma = 4\pi\rho/\lambda_w$.

- Increase of emittance and the energy spread results in suppression of the mode degeneration effect for the price of the gain reduction of the fundamental mode TEM_{00} mode.

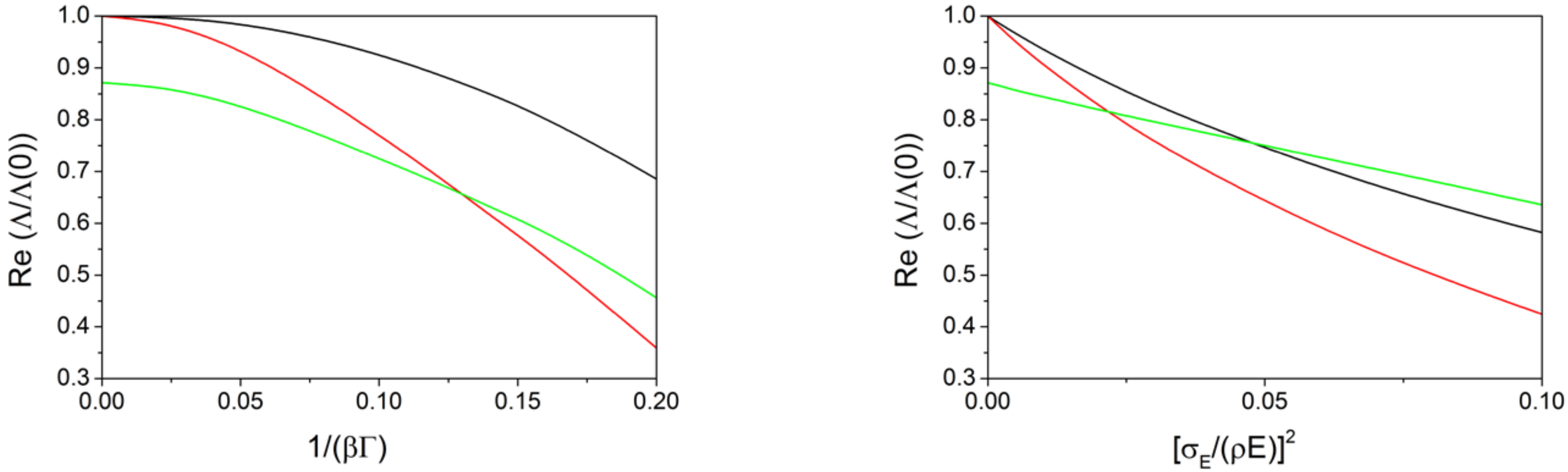

Suppression of the mode degeneration for B = 10

Outline

- General overview of coherence properties.
- Eigenmodes and eigenfunctions.
- Experience from FLASH.
- Optimized x-ray FEL.
- Coherence properties of the radiation from optimized x-ray FEL.
- Photon beam pointing stability.

FLASH

Energy	[GeV]	0.5-1.25	
Wavelength	[nm]	4.1-55 (FLASH1), 3.x-8.x (FLASH2)	
Pulse energy	[uJ]	10-500	
Rep. rate	[Hz]	5000	
Undulators			
	Period	Length	
FLASH1:	2.73 cm	27 m (6 x 4.5 m modules)	fixed gap
FLASH2:	3.14 cm	30 m (12 x 2 m modules)	variable gap

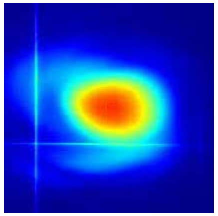

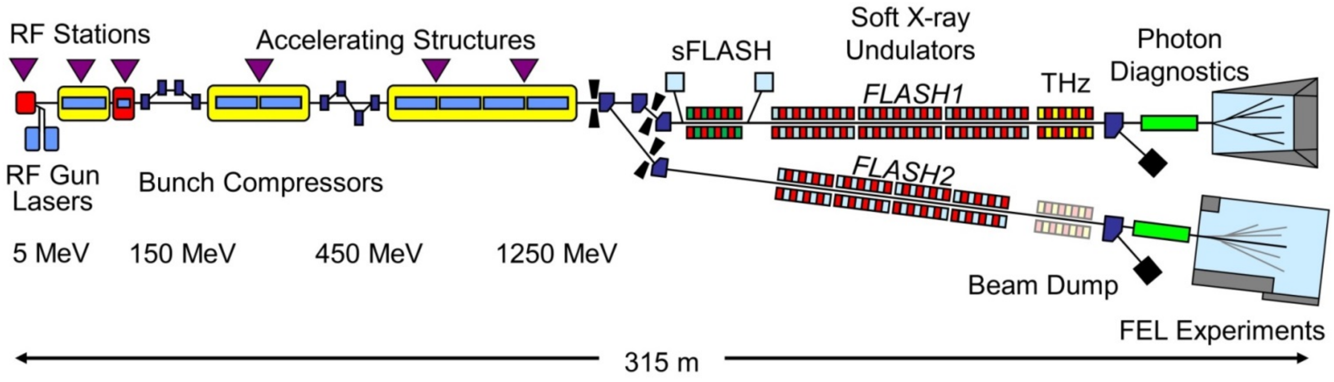

Observation at FLASH:

- The degree of transverse coherence is visibly less than unity in the post-saturation regime
- Transverse shape of the photon pulse is not stable.
- Pointing stability is not perfect.
- Pointing stability degrades for shorter photon pulses.

FLASH

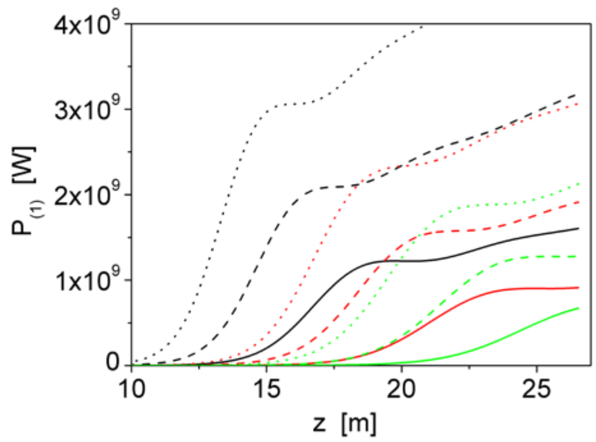

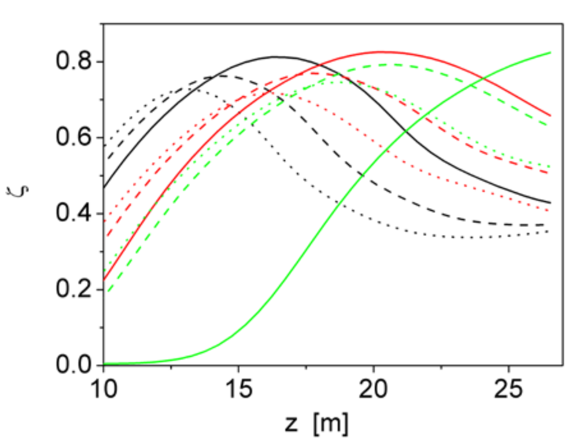

Two effects defines degradation of the transverse coherence at FLASH:

- Mode degeneration.
- Poor longitudinal coherence. The essence of the effect is a superposition of mutually incoherent fields produced by different longitudinally uncorrelated parts of the electron bunch. In the exponential gain regime this effect is relatively weak, but it prevents a SASE FEL from reaching full transverse coherence, even in the case when only one transverse eigenmode survives. In the deep nonlinear regime beyond FEL saturation, this effect can be strong and can lead to a significant degradation of the degree of transverse coherence.

FLASH

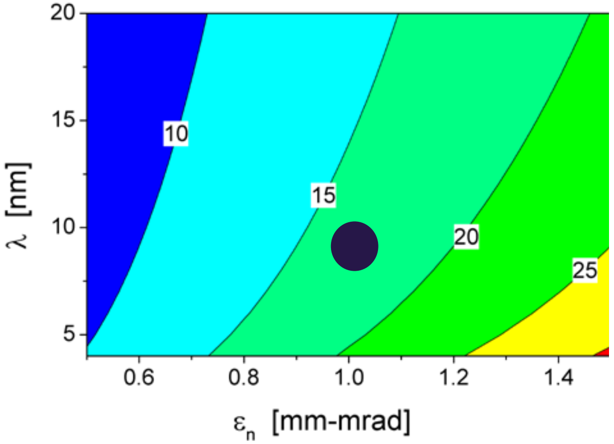

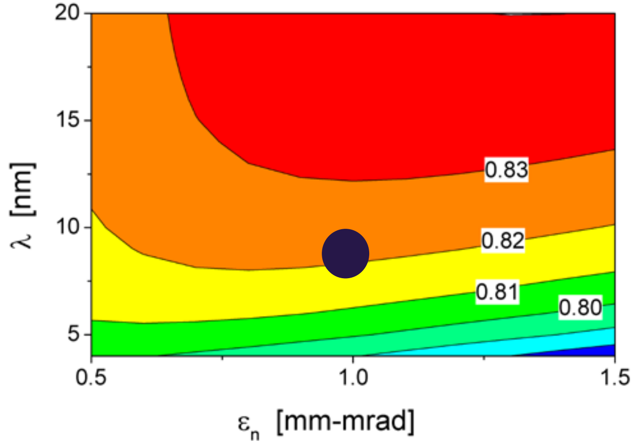

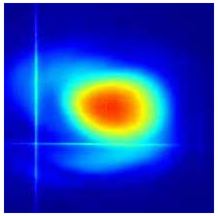

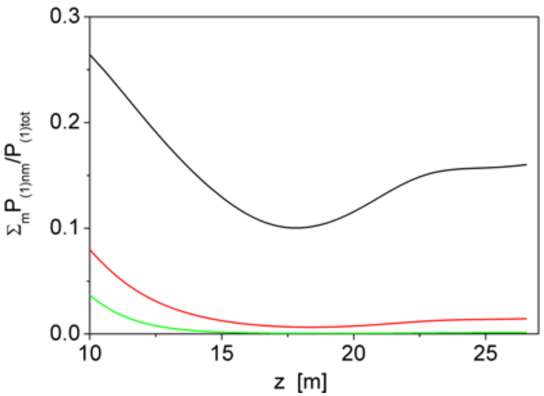

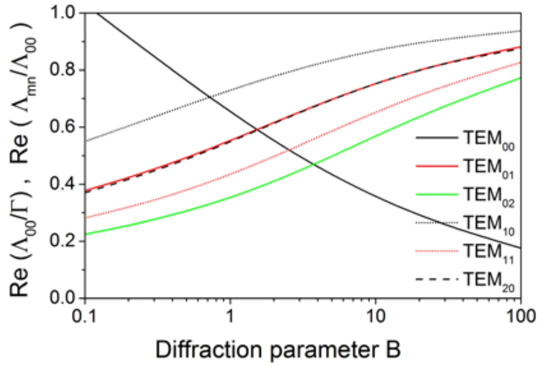

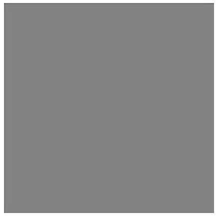

Parameter space of FLASH:

Large values of diffraction parameter (B = 10 - 25) and “cold” electron beam.

Mode degeneration effect is strong (gain of TEM10 mode is 0.8 – 0.83 of the fundamental TEM00).

Contribution of the first azimuthal mode to the total power is 10 to 15%.

Result: unstable shape and pointing of the photon pulse.

FLASH

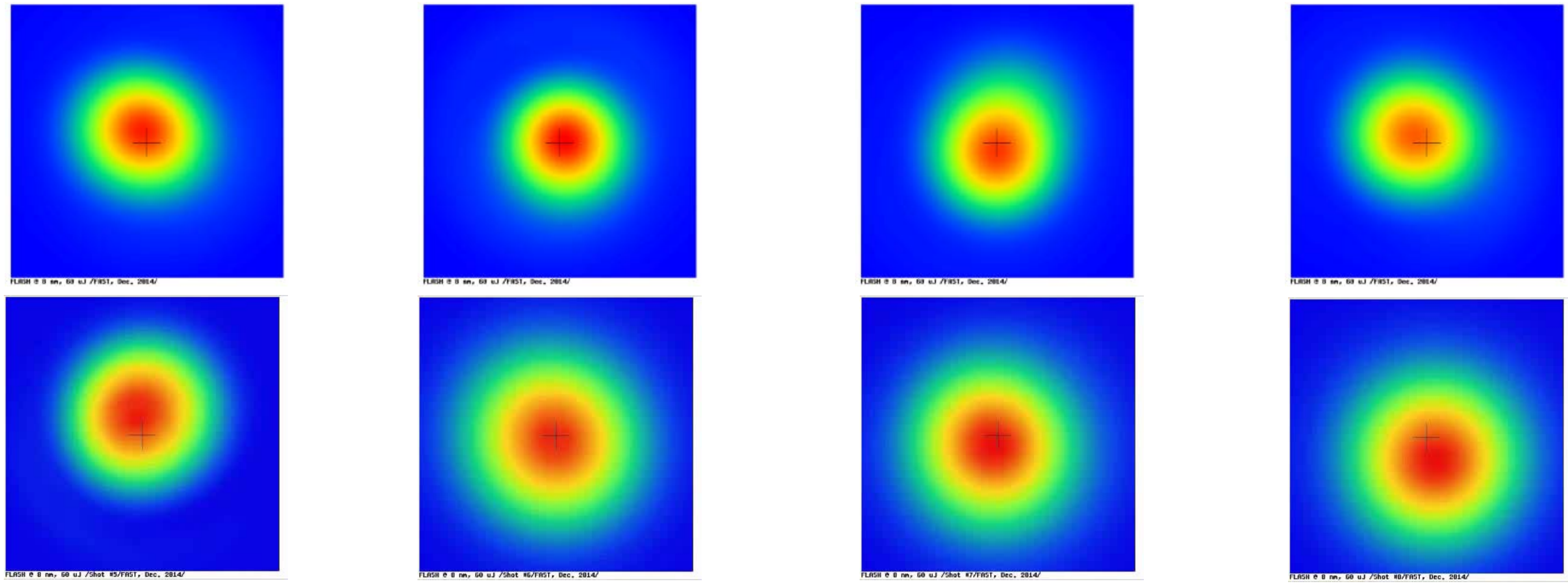

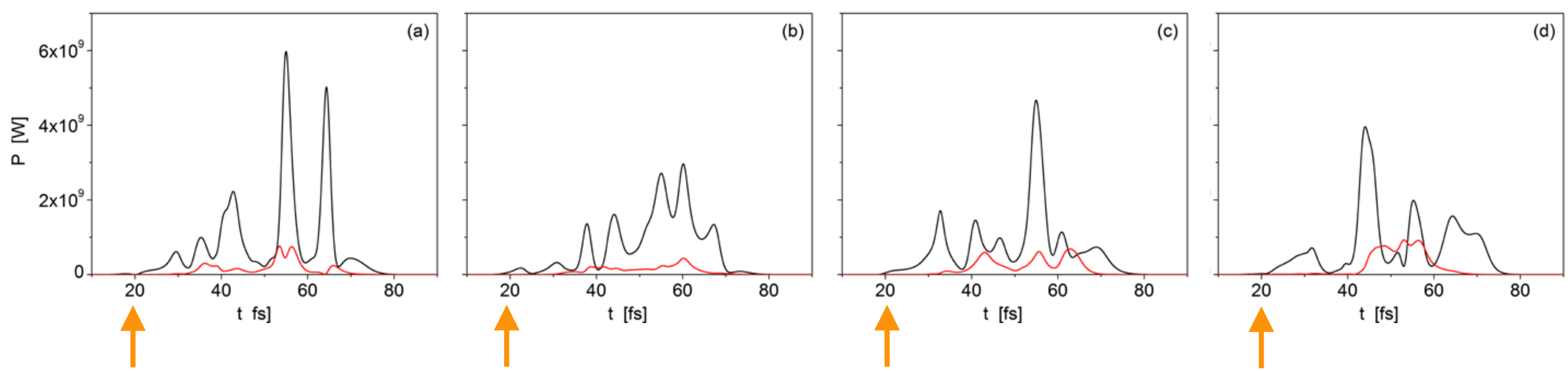

Evolution of the intensity distribution in the far zone along radiation pulse.

FLASH: recipes for improving transverse coherence

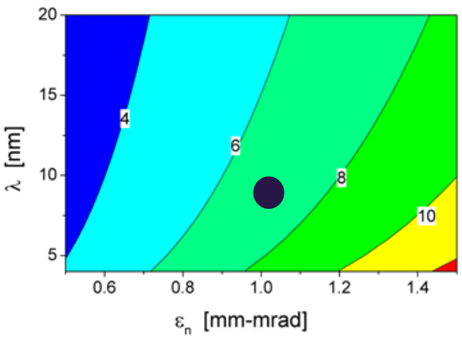

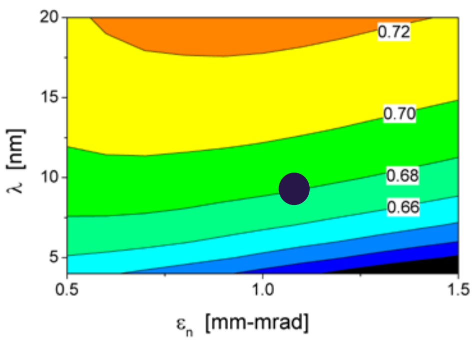

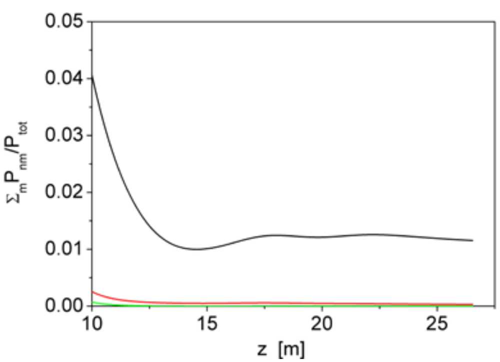

- To decrease the beam current such that saturation is achieved at the very end of the undulator. This would eliminate not only the degradation in the deep nonlinear regime, but would also improve the mode selection process because the diffraction parameter is then reduced while the velocity spread due to emittance is increased. Such a regime was realized at FLASH on user‘s demand, but it is not typical for the machine operation because the peak power is low due to a low peak current.

- One can also suppress the unwanted effects in the deep nonlinear regime by kicking the electron beam at the saturation point (or, close to it) when the peak current is high. Then one can still have a high power and an improved (about 70-80%) degree of transverse coherence.

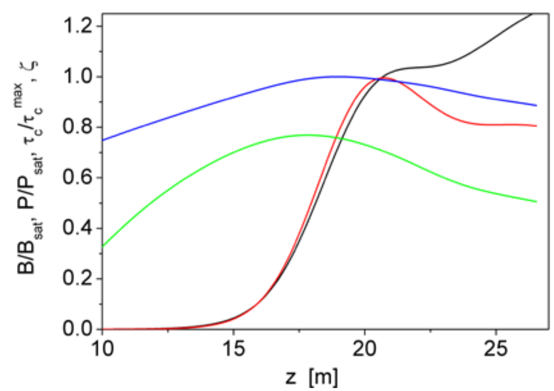

- Further improvement could be achieved by the reducing beta-function (thus improving the mode selection due two reduction of the diffraction parameter and increasing of the betatron motion parameter).

Outline

- General overview of coherence properties.
- Eigenmode and eigenfunctions.
- Experience from FLASH.
- Optimized x-ray FEL.
- Coherence properties of the radiation from optimized x-ray FEL.
- Photon beam pointing stability.

Optimized x-ray FEL

- Typical procedure of optimization of short wavelength SASE FEL consists in optimization for the maximum gain of the fundamental (TEM_{00}) beam radiation mode. This case is referred as optimized x-ray FEL.

- Gain and optimum beta function in the case of small energy spread:

$$L_{\mathrm{g}} \simeq 1.67 \left(\frac{I_A}{I}\right)^{1/2} \frac{(\epsilon_n \lambda_{\mathrm{w}})^{5/6}}{\lambda^{2/3}} \frac{(1+K^2)^{1/3}}{K A_{JJ}} \;, \qquad \beta_{\mathrm{opt}} \simeq 11.2 \left(\frac{I_A}{I}\right)^{1/2} \frac{\epsilon_n^{3/2} \lambda_{\mathrm{w}}^{1/2}}{\lambda K A_{JJ}} \;.$$

- Application of similarity techniques to the FEL equations gives elegant result: characteristics of SASE FEL written down in the normalized form are functions of two parameters, ratio of geomtrical emittance to the wavelength, and the number of electrons in the volume of coherence:

$$\hat{\epsilon} = 2\pi\epsilon/\lambda \;, \qquad N_{\mathrm{c}} = I L_{\mathrm{g}} \lambda/(e\lambda_{\mathrm{w}} c) \;.$$

- Dependence of the FEL characterestics on N_{c} is very slow, in fact, logarithmic. Approximately, with logarithmic accuracy they depend only on $\hat{\epsilon}$.

- In fact, the diffraction parameter B and the betatron oscillation parameter k_β are:

$$B \simeq 13 \times \hat{\epsilon}^{5/2} \;, \qquad k_\beta \simeq 0.154/\hat{\epsilon}^{3/2}$$

Optimized x-ray FEL

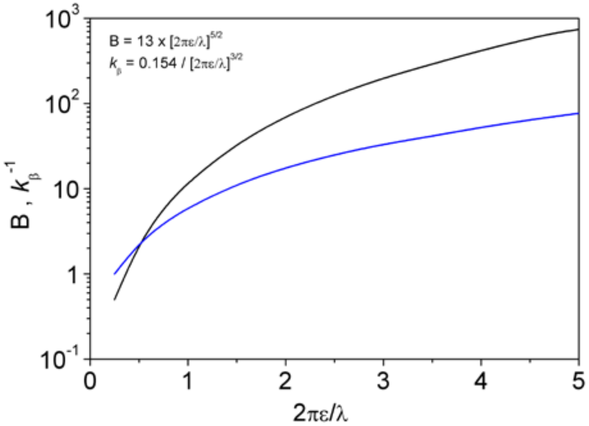

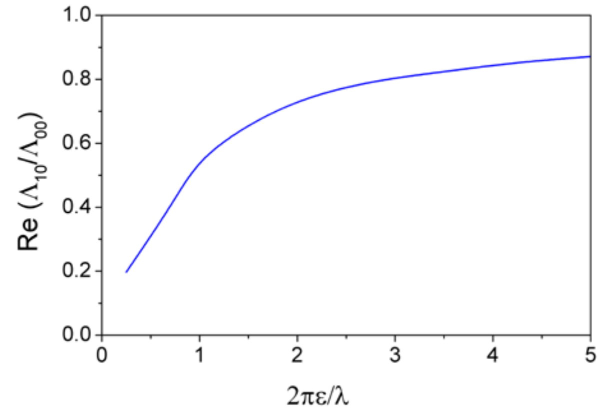

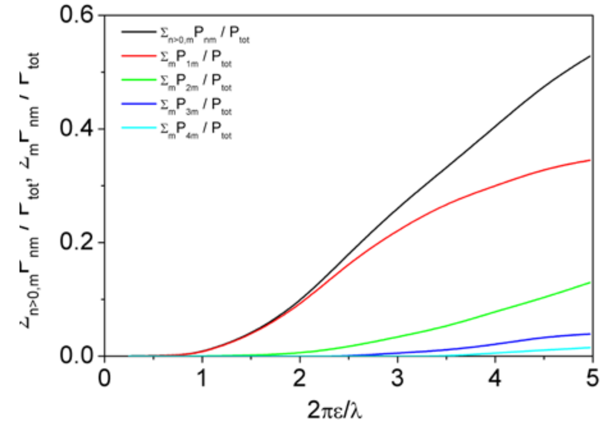

- Features of optimized x-ray FEL for parameter space $2\pi\epsilon/\lambda > 1$:
- Large values of the diffraction parameter.
- Mode degeneration effect takes place.
- Significant contribution of higher azimuthal radiation modes.
- Poor spatial coherence.
- Complicated and essentially non-gaussian field distributions across slices of the radiation pulse.
- Poor pointing stability of the radiation.

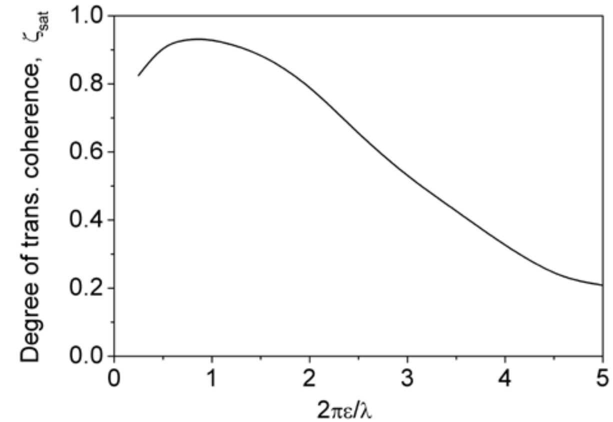

Optimized x-ray FEL

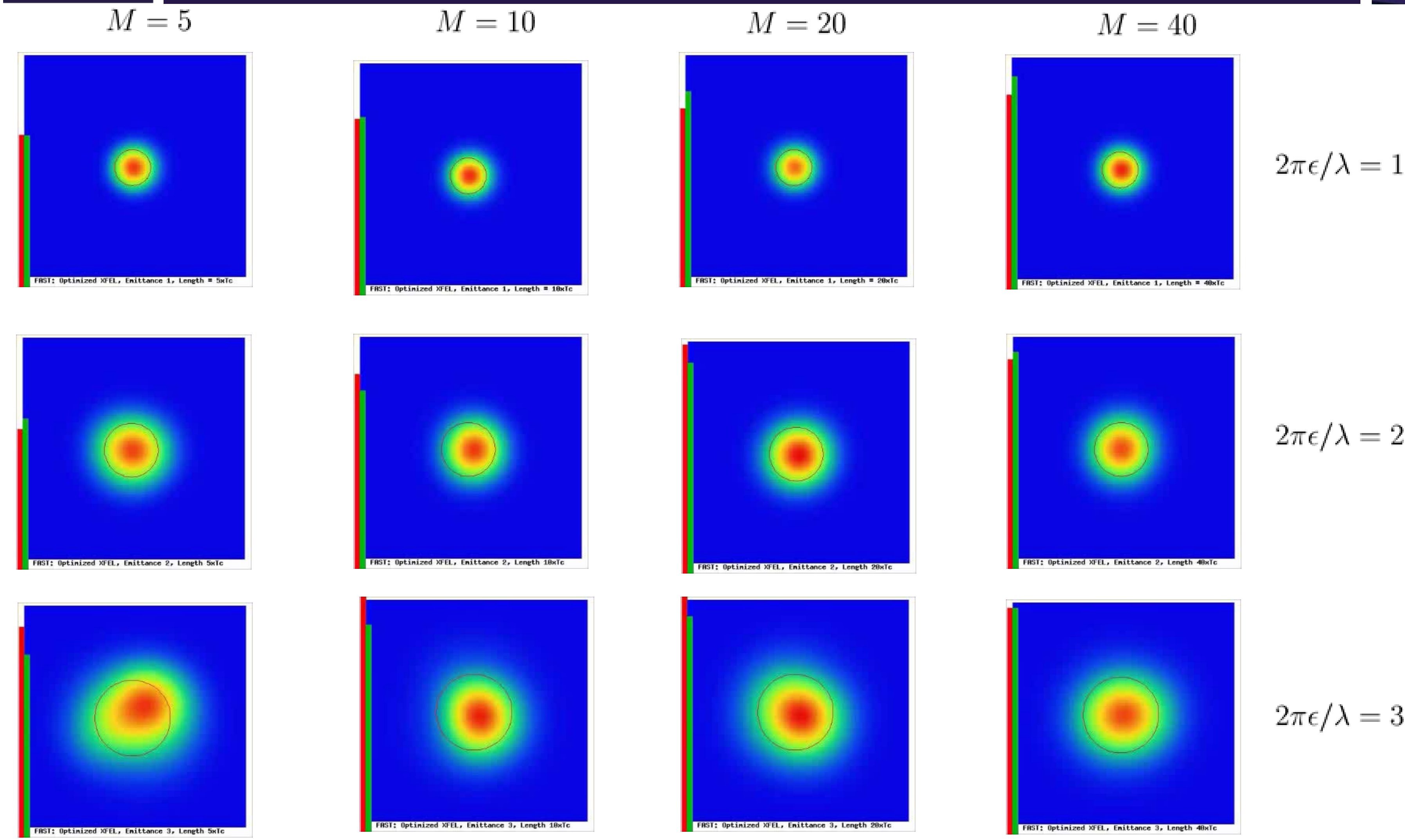

- Single shot photon beam images for pulse durations $T = M \times \tau_c = 5$, 10, 20, and 40, and emittances $2\pi\epsilon/\lambda = 1$, 2, and 3.

Optimized x-ray FEL

$2\pi\epsilon/\lambda = 1$ $2\pi\epsilon/\lambda = 2$ $2\pi\epsilon/\lambda = 3$ $2\pi\epsilon/\lambda = 4$

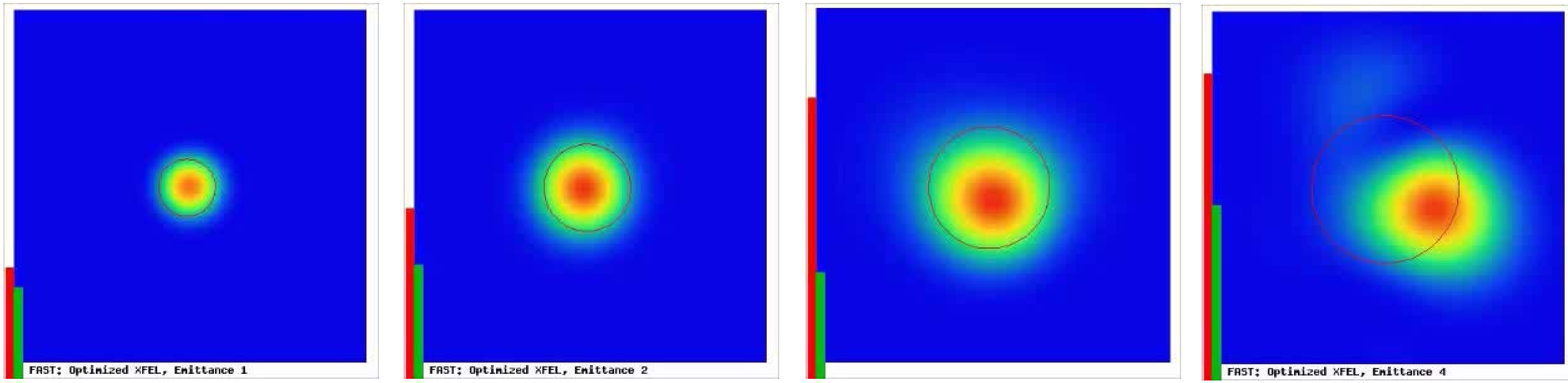

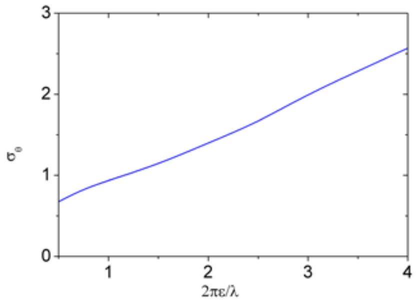

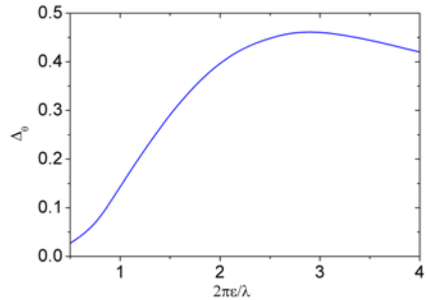

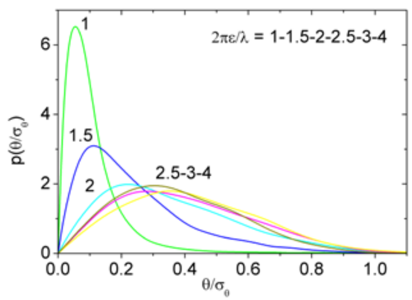

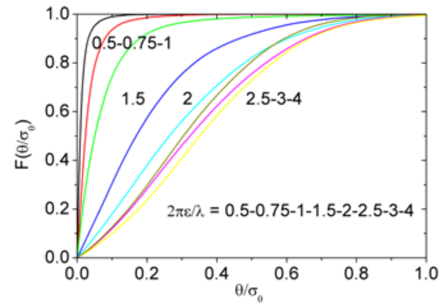

- Slice intensity along radiation pulse in the far zone for $2\pi\epsilon/\lambda = 1, 2, 3, 4$.
- Averaged rms size of the photon beam σ_θ in units of $\lambda/(2^{3/2}\pi\sigma)$.
- rms deviation of the photon beam center of gravity Δ_θ in units of averaged rms size of the photon beam.
- Probability distribution of the photon beam center of gravity, $P(\theta/\sigma_\theta)$.
- Cumulative probability distribution, $F(\theta/\sigma_\theta)$.

	LCLS	SACLA	EXFEL	SWISS FEL	PAL XFEL
Energy [GeV]	13.6	8.0	17.5	5.8	10
Wavelength [A]	1.5	0.6	0.5	0.7	0.6
ϵ_n [mm-rad]	0.4	0.4	0.4	0.4	0.4
$\hat{\epsilon} = 2\pi\epsilon/\lambda$	1	2.7	1.5	3.4	2.1

Summary

- When transverse size of the electron beam exceeds diffraction limit, the mode competition effect does not provide the selection of the fundamental FEL mode, and higher order spatial modes start to contribute to the radiation power.
- The consequence of interference of statistically independent spatial modes are:

  - Degradation of transverse coherence;

  - Fluctuations of the shape and pointing stability of the photon beam (both, slice and full shot).

  - Complicated and essentially non-gaussian field distributions across the slice.
- These effects stems from fundamental origin -- start-up of the amplification process from the shot noise in the electron beam. They become pronouncing at the very early stage of the degradation of the transverse coherence due to the growing contribution of the azimuthally non-symmetric modes.

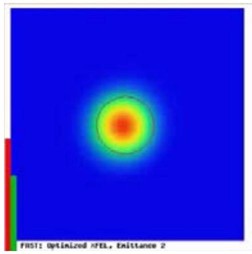

- X-ray FELs operating at short wavelengths will demonstrate degradation of the slice field patterns and the pointing stability with the increase of the parameter $2\pi\varepsilon/\lambda > 1$.

Thank you very much for your attention!

Backup slides

Related papers

The talk is essentially based on the following publications:

- E.A. Schneidmiller and M.V. Yurkov, Coherence properties of the radiation from FLASH, J. Mod. Optics (2015).
- E.A. Schneidmiller and M.V. Yurkov, Proc. FEL 2015 Conference, Fundamental Limitations of the SASE FEL Photon Beam Pointing Stability.

References for further reading:

Coherence properties of the radiation from SASE FEL:

- E.L. Saldin, E.A. Schneidmiller, and M.V. Yurkov, Statistical properties of radiation from VUV and X-ray free electron lasers, Optics Communications 148(1998)383.
- E.L. Saldin, E.A. Schneidmiller, and M.V. Yurkov, Diffraction effects in the self-amplified spontaneous emission FEL, Optics Communications 186(2000)185.
- E.L. Saldin, E.A. Schneidmiller, and M.V. Yurkov, Coherence properties of the radiation from X-ray free electron laser, Optics Communications, 281(2008)1179.
- E.L. Saldin, E.A. Schneidmiller, and M.V. Yurkov, Output power and degree of transverse coherence of X-ray free electron lasers, Optics Communications, 281(2008)4727.
- E.L. Saldin, E.A. Schneidmiller, and M.V. Yurkov, Statistical and coherence properties of radiation from x-ray free-electron lasers, New J. Phys. 12 (2010) 035010
- E.A. Schneidmiller, and M.V. Yurkov, Proc. FEL 2012 Conference, Coherence Properties of the Odd Harmonics of the radiation from SASE FEL with planar undulator.

FEL radiation modes:

- E.L. Saldin, E.A. Schneidmiller, and M.V. Yurkov, The Physics of Free Electron Lasers (Springer-Verlag, Berlin, 1999).
- E.L. Saldin, E.A. Schneidmiller and M.V. Yurkov, On a linear theory of an FEL amplifier with an axisymmetric electron beam, Opt. Commun. (1993)272-290.
- E.L. Saldin, E.A. Schneidmiller and M.V. Yurkov, The general solution of the eigenvalue problem for a high-gain FEL, Nucl. Instrum. and Methods A 475 (2001) 86-91.

Optimized SASE FEL

- E.L. Saldin, E.A. Schneidmiller and M.V. Yurkov, Design formulas for short-wavelength FELs , Opt. Commun. 235 (2004)415-420.
- E.A. Schneidmiller and M.V. Yurkov, Harmonic lasing in x-ray free electron lasers, PhysRevSTAB.15.080702.

Optimized x-ray FEL

Saturation length:

$$\hat{L}_{\mathrm{sat}} = \Gamma L_{\mathrm{sat}} \simeq 2.5 \times \hat{\epsilon}^{5/6} \times \ln N_{\mathrm{c}} \ ,$$

FEL efficiency:

$$\hat{\eta} \ = \ P/(\bar{\rho} P_{\mathrm{b}}) \simeq 0.17/\hat{\epsilon} \ ,$$

Coherence time and rms spectrum width:

$$\hat{\tau}_{\mathrm{c}} \ = \ \bar{\rho}\omega\tau_{\mathrm{c}} \simeq 1.16 \times \sqrt{\ln N_{\mathrm{c}}} \times \hat{\epsilon}^{5/6} \ , \qquad \sigma_{\omega} \simeq \sqrt{\pi}/\tau_{\mathrm{c}} \ .$$

Degree of transverse coherence:

$$\zeta_{\mathrm{sat}} \ \simeq \ \frac{1.1\hat{\epsilon}^{1/4}}{1 + 0.15\hat{\epsilon}^{9/4}} \ ,$$

Degeneracy parameter:

$$\hat{\delta} \ = \ \hat{\eta}\zeta\hat{\tau}_{\mathrm{c}}$$

Brilliance:

$$B_r \ = \ \frac{\omega d\dot{N}_{ph}}{d\omega} \frac{\zeta}{\left(\frac{\lambda}{2}\right)^2} = \frac{4\sqrt{2}c}{\lambda^3} \frac{P_{\mathrm{b}}}{\hbar\omega^2}\hat{\delta} \ .$$

Normalizing parameters:

$$\Gamma \ = \ \left[\frac{I}{I_{\mathrm{A}}} \frac{8\pi^2 K^2 A_{\mathrm{JJ}}^2}{\lambda\lambda_{\mathrm{w}}\gamma^3}\right]^{1/2} \ , \qquad \bar{\rho} = \frac{\lambda_{\mathrm{w}}\Gamma}{4\pi} \ .$$

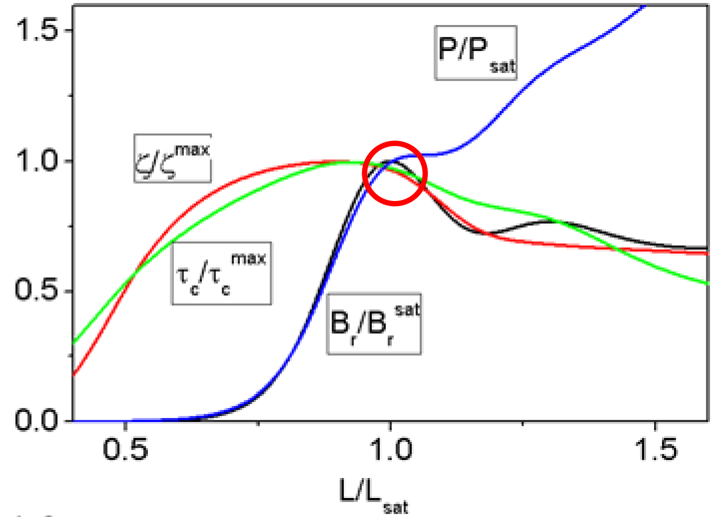

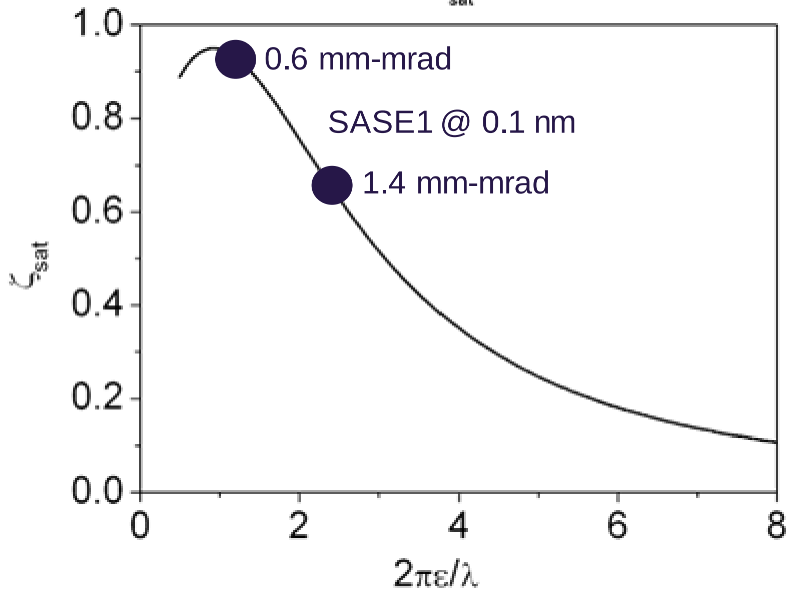

Properties of the radiation: Optimum tapered versus untapered case

- Practical example: European XFEL, SASE3, radiation wavelength 1.6 nm.
- General feature of tapered regime is that both, spatial and temporal coherence degrade in the nonlinear regime, but a bit slowly than for untapered case.
- Peak brilliance grows due to the growth of the radiation power, and reaches maximum value in the middle of tapered section. Benefit in the peak brilliance is about factor of 3 with respect to untapered case.

- Spatial corellations and degree of transverse coherence:

$$\gamma_1(\vec{r}_\perp, \vec{r\prime}_\perp, z, t) = \frac{\langle \tilde{E}(\vec{r}_\perp, z, t)\tilde{E}^*(\vec{r\prime}_\perp, z, t)\rangle}{\left[\langle|\tilde{E}(\vec{r}_\perp, z, t)|^2\rangle\langle|\tilde{E}(\vec{r\prime}_\perp, z, t)|^2\rangle\right]^{1/2}} ,$$

$$\zeta = \frac{\int |\gamma_1(\vec{r}_\perp, \vec{r\prime}_\perp)|^2 I(\vec{r}_\perp) I(\vec{r\prime}_\perp)\, \mathrm{d}\,\vec{r}_\perp\, \mathrm{d}\,\vec{r\prime}_\perp}{\left[\int I(\vec{r}_\perp)\, \mathrm{d}\,\vec{r}_\perp\right]^2} ,$$

- Temporal corellations and coherence time:

$$g_1(\vec{r}, t - t') = \frac{\langle \tilde{E}(\vec{r}, t)\tilde{E}^*(\vec{r}, t')\rangle}{\left[\langle|\ \tilde{E}(\vec{r}, t)\ |^2\rangle\langle|\ \tilde{E}(\vec{r}, t')\ |^2\rangle\right]^{1/2}} , \qquad \tau_c = \int\limits_{-\infty}^{\infty} |g_1(\tau)|^2\, \mathrm{d}\,\tau .$$

Power and brilliance

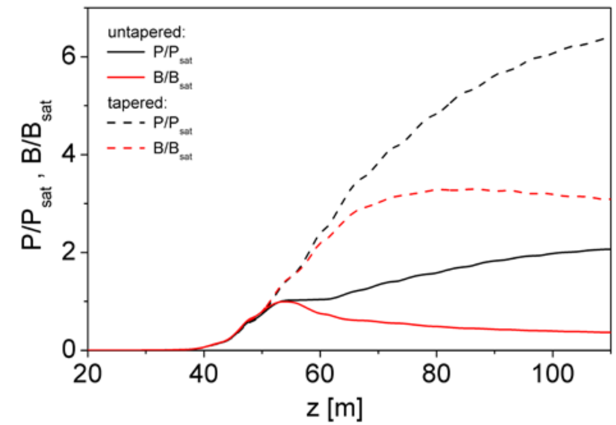

Degree of transverse coherence

Coherence time